DOE/NV/25946--526

Dynamic characterizations of an 8-frame, half-strip, high-speed x-ray microchannel plate imager

Ken Moy,[*a] Ming Wu,[♦a] Craig Kruschwitz,[a] Aric Tibbitts,[a] Matt Griffin,[a] and Greg Rochau[b]
[a]National Security Technologies, LLC, Las Vegas, NV, USA 89193;
[b]Sandia National Laboratories, Albuquerque, NM, USA 87185

ABSTRACT

High-speed microchannel plate (MCP)–based imagers are critical detectors for x-ray diagnostics employed on Z-experiments at Sandia National Laboratories (SNL) to measure time-resolved x-ray spectra and to image dynamic hohlraums. A multiframe design using eight half strips in one imager permits recordings of radiation events in discrete temporal snapshots to yield a time-evolved movie. We present data using various facilities to characterize the performance of this design. These characterization studies include DC and pulsed-voltage biased measurements in both saturated and linear operational regimes using an intense, short-pulsed UV laser. Electrical probe measurements taken to characterize the shape of the HV pulse propagating across the strips help to corroborate the spatial gain dependence.

Keywords: Microchannel plate, Z accelerator, time-resolved x-ray spectra, UV laser

1. INTRODUCTION

High-speed gated x-ray MCP[1]–based imagers are used internationally in diagnostics for research in high-energy-density physics (HEDP).[2-4] For HEDP research undertaken at the SNL Z accelerator[5-6] using dynamic hohlraums, such devices are critical imaging detectors deployed in multilayer mirror (MLM[7]) filtered pinhole cameras and time- and space-resolved elliptical crystal (TREX[8-9]) diagnostics. Discrete images from the measurements taken with these diagnostics are used to unfold the spatial profile of the hohlraum temperatures to characterize the time history of emitted radiation.

The advent of a more intense x-ray source promised by the newly improved, refurbished SNL Z accelerator presents a need for higher speed and higher resolution imaging diagnostics. To meet this demand, we developed an improved 8-frame, half-strip MCP design that retains the same footprint of previous imagers and is mechanically packaged to maintain compatibility with the mounting flange and film-pack used in those diagnostics.

[*] moykj@nv.doe.gov; phone 1 805 681-2284
[♦] wum@nv.doe.gov; phone 1 505 663-2030

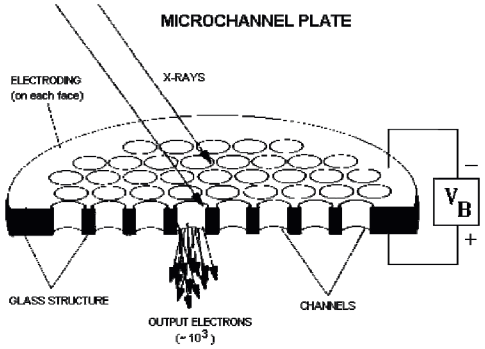

Fig. 1. MCP structure.

2. MCP CAMERA SYSTEM DESCRIPTION

The MCPs used in the camera are constructed from lead glass matrices of microchannel pores tilted at a slight 8º from normal. Functionally, incident radiation (energetic photons or charged particles) strikes the pore wall entrances to release secondary electrons (Figure 1). Under the influence of a large electric field, produced by an applied voltage, the electrons cascade down the length of the channels to produce more secondaries. On exit, the output electrons can be measured in an electrical circuit or strike a phosphor to produce light for recording.

For our structure, conductive layers are deposited on a circular 40-mm-diameter MCP manufactured by Burle, Inc., to provide the eight frames. These layers are formed by physical vapor deposition using materials and thicknesses of: 75 Å Cr, 5000 Å Cu, 75 Å Cr, and 1000 Å Au. The entrance surface is coated with eight 8-mm-wide half strips carefully separated by 1-mm spacing, with four half strips each about 25-mm long, and the other four half strips each about 22-mm long (Figure 2). These half strips are coated at 60º from the surface normal, while the exit surface is coated uniformly with the same conductive layers at 45°. The structural parameters are:

- MCP diameter: 40 mm, 8 half strips: 4 (8 mm × 25 mm) and 4 (8 mm × 22 mm)
- MCP pores: diameter D = 10 μm, Length L = 460 μm, bias angle = 8º, L/D = 46, L/4D ~ 11.5

Using the discrete dynode model[10], the electron gain is found to be:

$$G = \left(\frac{V}{V_o}\right)^{L/4D} \approx \left(\frac{V}{V_o}\right)^{11.5}$$

V: applied voltage
V_o: minimum "turn-on" voltage

The electrons emerge from the MCP pores to strike a P43 phosphor with luminescence peaked at 545 nm that is well-suited for film recording. The P43 is deposited by Lexel Imaging Systems onto a fiber-optics faceplate (Block Press BLE59-6, Incom Inc.) and over-coated by a thin layer of indium-tin-oxide (ITO) by Deposition Research Laboratory, Inc., using their 70CHTS procedure. The ITO provides a conductive base for an applied voltage, either pulsed or DC, to accelerate the emerging electrons onto the phosphor.

A transmission line design is laid on a flexible circuit board to transfer the 50-Ω voltage pulse onto the ~12-Ω strip input. The half strip's opposite end is open circuited to take advantage of the large pulse reflection that effectively adds to the incident pulse amplitude to provide a higher gain. For our eight half strips, the open-circuit ends terminate at the center of the MCP.

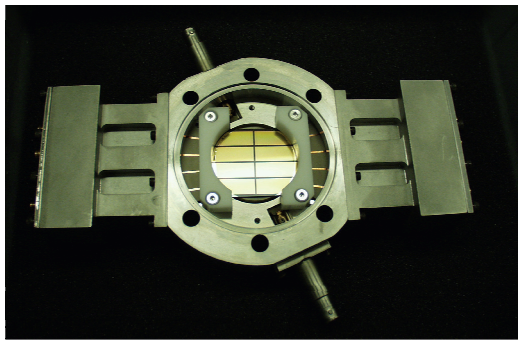

Fig. 2. 8-frame, half-strip MCP framing camera.

An important part of this MCP–based imaging system is found in the 8-channel, high-voltage pulser system developed and fabricated by Kentech to our design specifications. As shown in Figure 3, all eight pulser modules are integrated onto a compact standard 19" rack mount. Pulse-forming networks in these modules can be set individually, allowing experimenters to obtain a variety of waveforms for the detector. This system is interfaced to a PC with LabVIEW software (Figure 4) for full operational control to track and set the DC bias, gate widths, and gate-delay time for each module. These capabilities carry a broad range of operational controls to the imaging system to allow a wide range of uses and on-the-fly flexibility.

Fig. 3. Compact Kentech CSP3 pulser system.

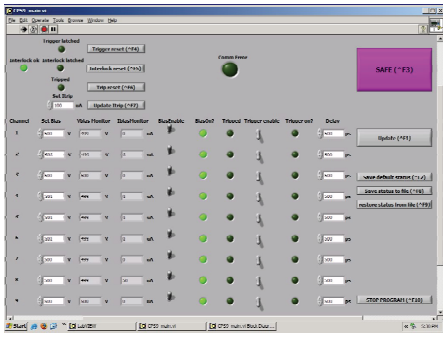

Fig. 4. Pulser system control and automation software.

Many engineering features in this camera design help to enhance its reliability, sensitivity, and gain uniformity. For example, side-launching the striplines to a pusher bar not only improves the impedance match but also reduces the mechanical stress on the MCP. The etched waferboard extends from the stripline to the feed-through, reducing the number of connections and removing the need for an epoxy fill. The camera is also designed to permit the phosphor HV bias to be pulsed with a separate connector to monitor this pulsed waveform. Pulse-biasing the phosphor helps to minimize breakdown-induced light contamination and potential device failure due to arcing; these events have occurred in MCP imagers fielded on past Z-experiments. In addition, pulse-biasing the phosphor up to a few microseconds (more than sufficient to cover the “turn-on” measurement time for Z-experiments) also permits a higher-peak applied voltage to increase image sharpness and intensity.

3. CHARACTERIZATION USING A UV SHORT-PULSE LASER

Characterization of the MCP detector was conducted at the short-pulse laser (SPL) facility at Livermore Operations (LO). This facility provides short-pulse UV irradiation suitable for characterizing the MCP’s performance as a function of pulsed and DC bias, pulsed phosphor bias, and investigation of gate profile/time response and gain uniformity.

3.1 Experiment setup and image processing

Schematics of optical, electronic, and trigger setups employed at the SPL are shown in Figure 5. The laser output wavelength is 200 nm, amplified from a frequency-quadrupled 100-fs Ti:Sapphire seed laser operated at 800 nm. The 200-nm laser pulse has ~200-μJ beam energy with pulse duration of <500 fs. The beam passes through a neutral density filter (CVI Melles Griot, UVDA high-energy dielectric UV attenuator), a diffuser (Physical Optics Corp., UV holographic diffuser with 1° divergence), and a homogenizer (Coherent Inc.) in order to expose the entire MCP active area to a uniform beam intensity. The beam intensity is varied by inserting selectable combinations of neutral density filters. The beam energy is monitored by a laser power meter (LaserProbe, 7620 Energy Meter), and the beam timing is monitored using a diamond photo-conductive detector (PCD) with ~200-ps rise time.

The trigger input for the experiments was taken from the laser, and sent to a Kentech delay generator to select a suitable delay to trigger the timing synchronizer. The outputs of the synchronizer triggered the Avtech pulser, CCD camera, laser power meter, and shutter controller. The Avtech pulser output was sent through a 50-Ω power divider to trigger the Kentech 8-channel HV pulser system and the Tektronix DPO/DSA71604 (16 GHz/50 GS/s).

A rectangular coherent fiber plug (36 mm × 40 mm × 152 mm, quality area of 34 mm × 38 mm) built by Incom was used to couple the MCP phosphor to a computer-controlled CCD readout camera. The glass fibers in the plug are 4.5 μm in diameter. The readout camera is a custom-designed Spectral Instruments 800 series with a KAF-16801E class-2 chip, and a high-performance CCD image sensor with 4096 × 4096 (9-μm) photo-active pixels.

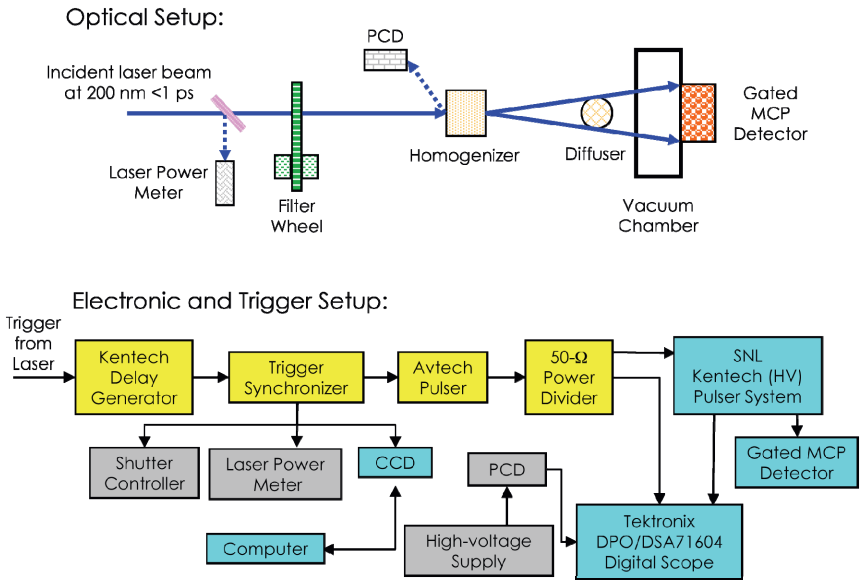

Fig. 5. Optical, electronic, and trigger setup for the dynamic characterizations at the SPL facility.

The bias voltage applied to each strip can be either a negative DC voltage or a negative HV pulse combined with a DC component. Sensitivity and saturation effects of the MCP in DC mode were measured by varying the DC bias voltage and laser flux. MCP gate profile and gain uniformity in pulsed mode were studied by varying the laser flux after the laser and HV pulses were synchronized and overlapped positions of interest on the half strip. Five images were recorded at each delay setting, with the net intensity obtained by averaging a selected area from these images.

For MCP tests with the phosphor in pulsed operations, the phosphor was biased with a 2-μs, +3000-V pulse with respect to the MCP back/exit surface.

3.2 DC performance with UV laser source

To obtain the MCP sensitivity in the DC mode, the image intensity was averaged over eight half strips, irradiated with three laser shots for each DC bias setting. Each image was normalized by the laser energy of each shot. These measurements were repeated at variable laser fluxes to study response linearity and saturation.

Figure 6 shows the MCP sensitivity as a function of DC bias voltage from −300 to −900 V. The incident laser flux was varied from 1.44 μJ/cm^2 to 27 nJ/cm^2. At very low laser flux, the relative sensitivity follows very well as expected from the discrete dynode gain model, which has an 11.5 power dependence of DC bias voltage. But as the laser flux is increased, the gain deviates from the model's prediction, changing from about a $G{\sim}V^{11}$ to a $G{\sim}V^{9}$ dependence before the onset of hard saturation. These results indicate that a weak saturation can change the exponent of gain with voltage and that a strong saturation leads to a gain plateau. While the weak saturation may be due to high electron numbers present in the channel at a given time (space-charge effect), the strong saturation is a wall-charging effect. These results showed that it is critical to determine the response linearity of the MCP detector in terms of laser power before dynamic characterization in pulsed mode is performed.

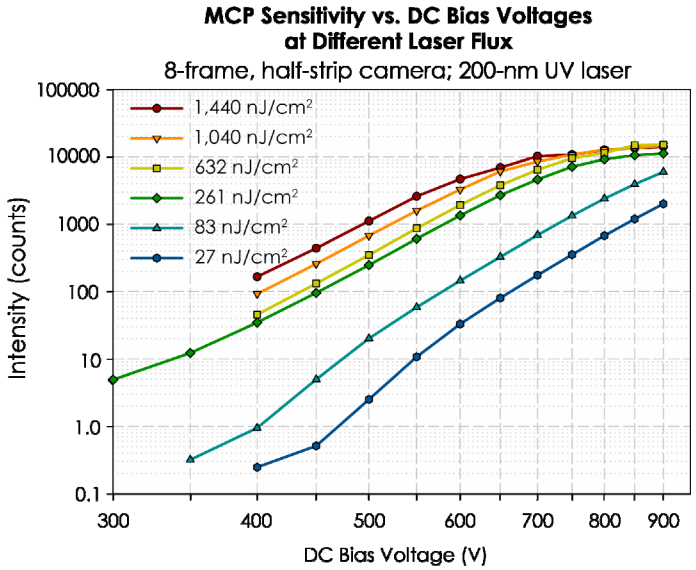

Fig. 6. MCP DC sensitivity under 200-nm, 500-fs laser radiations measured at the SPL facility.

3.3 Pulsed phosphor

For HEDP applications where our imager is required to capture a high-speed event without much image blur, the width of the voltage pulse applied to the MCP strip is in the sub-nanosecond to nanosecond range. Operating the phosphor in pulsed mode can limit or prevent late time vacuum and plasma discharge effects that can result in deleterious background light noise or even device malfunction. Pulsed phosphor operations should increase the reliability of the MCP imagers. Figure 7 shows MCP detector sensitivity vs. the pulse width of the phosphor bias. The MCP strips were biased at a constant −650 VDC, and the phosphor was triggered by a variable +3-kV pulse from a DEI pulser. The MCP sensitivity remained constant from DC to 0.6-μs pulse width. Below 0.6 μs, the sensitivity reduced linearly about 20% at 0.2 μs.

Figure 8 shows MCP detector sensitivity vs. pulse amplitude of the phosphor bias. Due to the small (<1-mm) gap between the MCP and the phosphor, for DC voltage bias, the phosphor is fixed at +3-kV DC to avoid arcing. With the phosphor pulsed at +5 kV and 2 μs, the detector sensitivity increased by ~2X and operated robustly without problems.

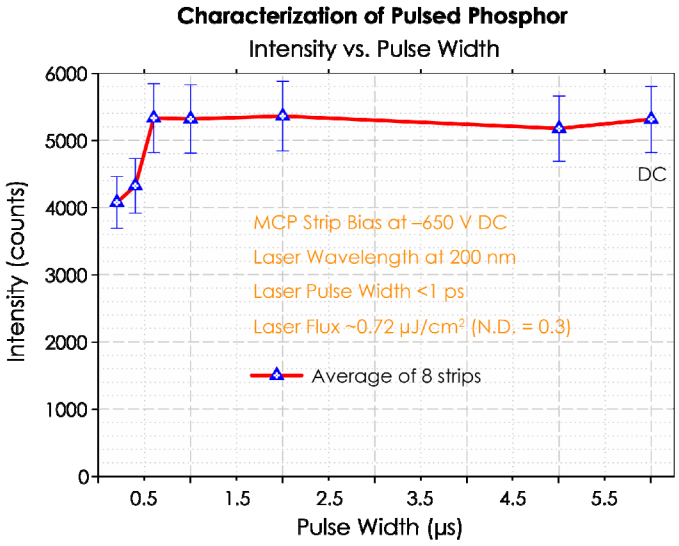

Fig. 7. MCP DC sensitivity vs. pulse width of phosphor bias.

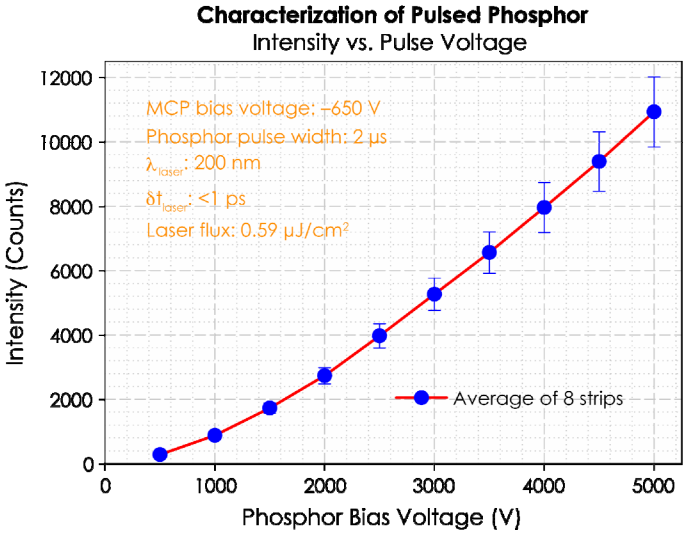

Fig. 8. MCP DC sensitivity vs. pulsed HV on the phosphor.

The MCP detector sensitivity in pulsed mode vs. the pulsed phosphor voltage was also measured with the half strips biased using the 8-channel Kentech pulser system. Due to the time jitter between the laser and HV pulses on the MCP half strips, it is necessary to monitor the delay for each shot using a 16-GHz, 50-GS/sec (Tektronix DPO/DSA71604) oscilloscope. Five data points were taken at each voltage setting to permit a nice statistical average. The general trend of MCP sensitivity as a function of applied phosphor voltage is similar for DC and pulsed mode operations.

3.4 Gate profile measurement

MCP detector images were recorded for a series of time delays between the laser and HV pulse on the MCP half strips. Five images were taken at each time delay, determined from the relative timing between the PCD signal and the voltage pulse. The 50% point of the rising edge on each of these signals can be determined to <10 ps. The gain at a specific time or location on the MCP strips is determined using the following procedure:

(1) subtract the CCD background from the image
(2) divide the background-subtracted image by the flat field of the beam profile taken with an applied DC voltage
(3) integrate a narrow region around the spatial location of interest to get the average intensity (in CCD counts)
(4) divide the average intensity by the measured laser energy.

Finally, the gate profiles are obtained by sorting the averaged intensities at locations of interest by the measured time delays with a bin width of 20 ps.

Figure 9 shows the gate profiles from three locations on a short half strip, and Figure 10 shows how the full width at half maximum (FWHM) varies along this strip. It is clear that the FWHM of the gate profile is almost a factor of two different between the beginning and end of the MCP half strip. The spatial dependence of the gate profiles is due to voltage waveform variations along the strip arising from reflections at the input junction due to impedance mismatch and the open-circuited end of the MCP half strip.

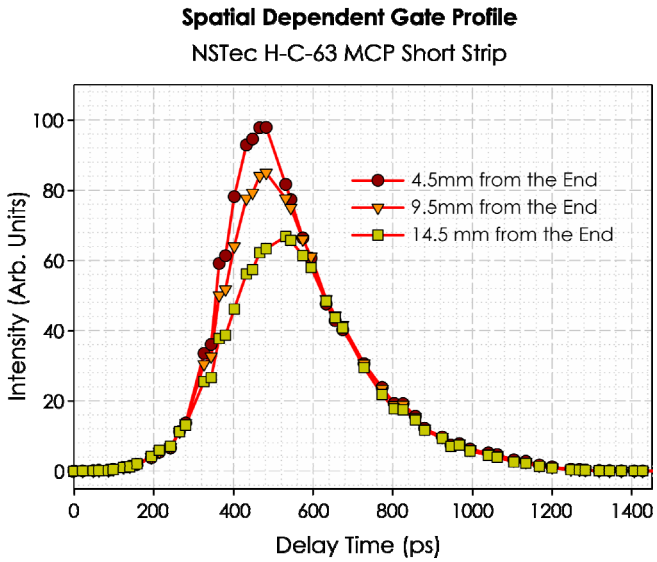

Fig. 9. Spatial-dependent gate profiles of NSTec H-C-63 MCP detector.

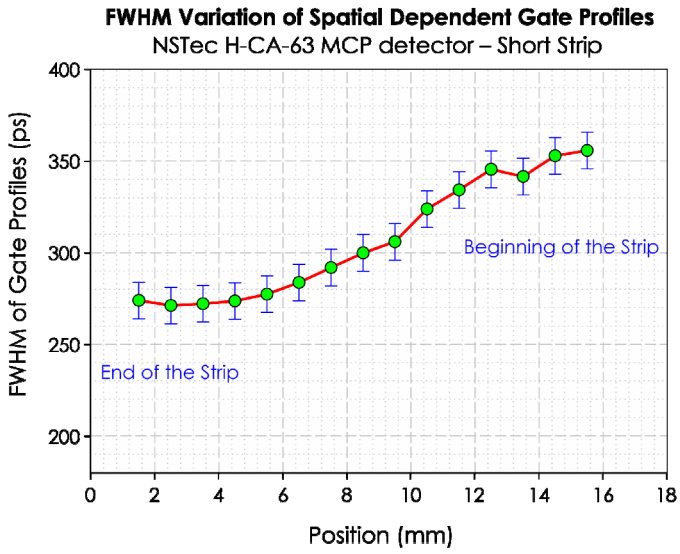

Fig. 10. FWHM measurements of spatial-dependent gate profiles.

3.5 Gain uniformity at pulsed mode

In general, flat-field characterization of an MCP imager under pulsed-mode operation is obtained by using an x-ray or UV-laser source, with a source-pulse length that is much longer than the optical gate profile. It is also possible to obtain the flat field using a short-pulse UV laser, a byproduct of spatial-dependent gate profile measurements where the incident radiation pulse width is much shorter than the MCP's optical gate profile width.

Sensitivity along the MCP half strip in pulsed mode when irradiated by a short-pulse laser is obtained by integrating the spatial-dependent gate profiles, as shown in Figure 11. In this regard, the flat field results from both a long-pulse and a short-pulse laser are identical. The advantage of using a long-pulse laser is that the flat-field measurement can be done using a single pulse. Since the measurements for a spatial-dependent gate profile is a necessary step in the characterization of the MCP imager, these results can be processed to obtain the spatial sensitivity along the strip, thus eliminating the need for long-pulse laser flat fielding. This 8-frame, half-strip MCP imager has <25% variation along the entire strip.

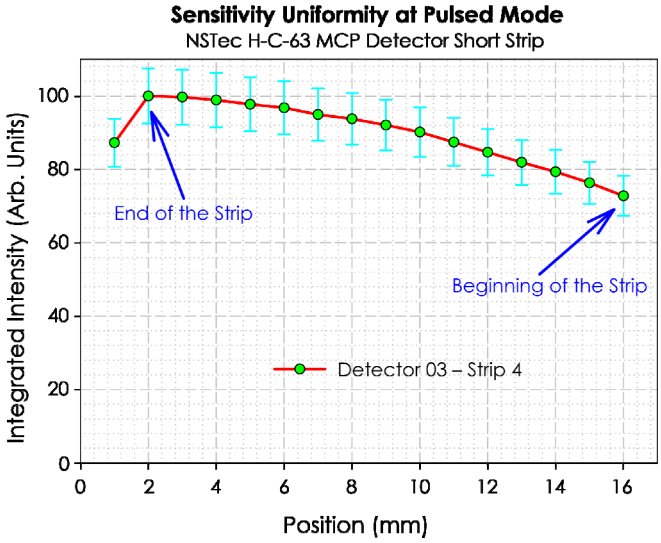

Fig. 11. Sensitivity uniformity of NSTec H-C-63 MCP detector in pulsed mode.

4. SURFACE-VOLTAGE MEASUREMENT ON MCP HALF STRIP

To fully understand the MCP's performance in pulsed mode, it is necessary to measure precisely the voltage waveform propagating on each half strip using a high-bandwidth electrical probe. The detailed experimental setup is shown in Figure 12, where a picoprobe GGB model-35, tipped with a 20-µm tungsten wire, is used to sample the surface of the MCP strip. The frequency response of the probe is DC to 26 GHz, and input resistance is 1.25 MΩ. The probe is mounted on a motorized x-y-z station, allowing it to be moved to any desired location on the strip with high accuracy.

Figure 13 shows the variations of a pulsed waveform propagated on a typical MCP half strip. The changes seen in the shape of the waveform are due to a superposition of the pulse reflections. Since the gain is extremely nonlinear, exponential to the applied voltage, the position-dependent gate profiles on the MCP strip are directly related to the net waveform variation along the strip. These profiles corroborate the gate profile measurements shown above in Section 3.4. Detailed Monte Carlo simulations to obtain gate profiles using the measured surface voltages along with comparisons to experimental results will be published in an upcoming issue of Review of Scientific Instruments.

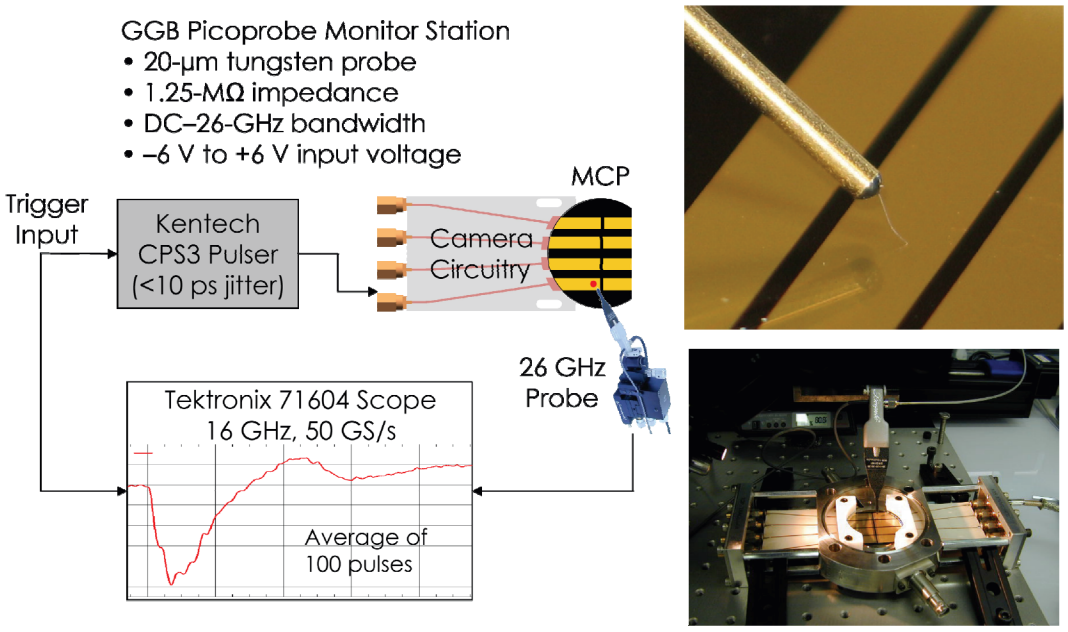

Fig. 12. Experimental setup of surface voltage measurement on the MCP strips using an active high-impedance probe.

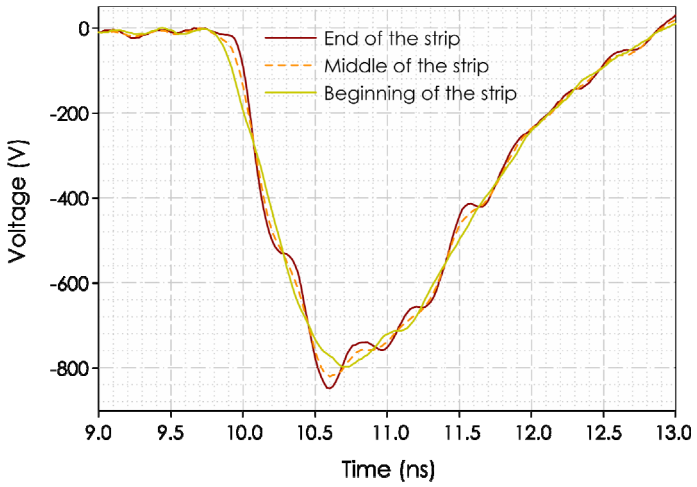

Fig. 13. Variation of voltage on MCP strip, NSTec H-CA-63 camera system.

5. SUMMARY AND CONCLUSION

We have developed and fully characterized a sub-nanosecond, 8-frame x-ray MCP imager that is controlled with a variable HV pulser to form a flexible imaging system. This imaging system was fielded on the inaugural experiment at the refurbished Z accelerator and returned eight high-quality spatially and temporally resolved images over a 10-ns window. Stemming from this initial success, especially noted by the high spatial- and temporal-resolution, additional MCP systems are earmarked to replace older designs.

6. ACKNOWLEDGMENTS

We would like to thank Bill Nishimura, Al Shellman, Dean Simmons, and other SPL staff members at our Livermore Operations for providing all necessary and timely support to ensure success with our UV measurements. Special thanks go to Mike Grover, Glen Anthony, and Tom Keenan for providing critical and timely support to redesign and salvage the fiber-optics image plug and assembly. The NSTec H-CA-63 camera system was designed, assembled, and tested at the Los Alamos Operations. We owe much gratitude to Nathan Joseph and Dale Crain for successfully fielding the camera system at the SNL Z facility. We acknowledge our Program Managers (Steve Goldstein, Dennis Barker), Darryl Droemer, and Tom Tunnell for their management support. Finally, much thanks to Kelly Streeton and Valerie Tyler for invaluable administrative support with preparation of this manuscript and presentation poster.

REFERENCES

[1]Kilkenny, J. D., Bell, P., Hanks, R., Power, G., Turner, R. E., and Wiedwald, J. , Rev. Sci. Instrum. 59, 1793 (1988).
[2]Masugata, K., Chishiro, E., Nakahama, N., Yatsui, K., and Tazima, T., Rev. Sci. Instrum. 68, 2046 (1997).
[3]Nash, T. J., Derzon, M. S., Chandler, G. A., Fehl, D., Leeper, R., Hurst, M., Jobe, D., Torres, J., Seaman, J., Lazier, S., Gilliland, T., and McGurn, J., Rev. Sci. Instrum. 70, 464 (1999).
[4]Oertel, J. T., Archuleta, T. N., and Shrank, L. S., Rev. Sci. Instrum. 72, 701 (2001).
[5]Spielman, R. B., Deeney, C., Chandler, G. A., Douglas, M. R., Fehl, D. L., Matzen, M. K., McDaniel, D. H., Nash, T. J., Porter, J. L., Sanford, T. W. L., Seamen, J. F., Stygar, W. A., Struve, K. W., Breeze, S. P., McGurn, J. S., Torres, J. A., Zagar, D. M., Gilliland, T. L., Jobe, D. O., McKenney, J. L., Mock, R. C., Vargas, M., Wagoner, T., and Peterson, D. L., Phys. Plasmas 5, 2105 (1998).
[6]Spielman, R. B., Long, F., Martin, T. H., Poukey, J. W., Seidel, D. B., Shoup, W., Stygar, W. A., McDaniel, D. H., Mostrom, M. A., Struve, K. W., Corcoran, P., Smith, I., and Spence, P., *Proceedings of the 10th IEEE Pulsed Power Conference*, 396, (1995).
[7]Jones, B., Deeney, C., Pirela, A., Meyer, C., Petmecky, D., Gard, P., Clark, R., and Davis, J., Rev. Sci. Instrum. 75, 4029 (2004).
[8]Lake, P. W., Bailey, J. E., Rochau, G. A., Gard, P., Petmecky, D., Bump, M., Joseph, N. R., Moore, T. C., Nielsen-Weber, L. B., Rev. Sci. Instrum. 77, 10F315 (2006).
[9]Bailey, J. E., Chandler, G. A., Slutz, S. A., Golovkin, I., Lake, P. W., MacFarlane, J. J., Mancini, R. C., Burris-Mog, T. J., Cooper, G., Leeper, R. J., Mehlhorn, T. A., Moore, T. C., Nash, T. J., Nielsen, D. S., Ruiz, C. L., Schroen, D. G., and Varnum, W. A., Phys. Rev. Lett. 92, 085002 (2004).
[10]Rochau, G. A., Bailey, J. E., Chandler, G. A., Nash, T. J., Nielsen, D. S., Dunham, G. S., Garcia, O. F., Joseph, N. R., Keister, J. W., Madlener, M. J., Morgan, D. V., Moy, K. J., and Wu, M., Rev. Sci. Instrum. 77, 10E323 (2006).